Published in final edited form as:
Sci Signal. ; 2(88): ra55. doi:10.1126/scisignal.2000304.

Differential Interactions of FGFs with Heparan Sulfate Control Gradient Formation and Branching Morphogenesis

Helen P. Makarenkova[1,2,*,†], **Matthew P. Hoffman**[3,*], **Andrew Beenken**[4], **Anna V. Eliseenkova**[4], **Robyn Meech**[2,5], **Cindy Tsau**[1], **Vaishali N. Patel**[3], **Richard A. Lang**[6], and **Moosa Mohammadi**[4,*]

[1]The Neurobiology Department, The Scripps Research Institute, La Jolla, CA 92037, USA

[2]The Neurosciences Institute, San Diego, CA 92121, USA

[3]Laboratory of Cell and Developmental Biology, National Institute of Dental and Craniofacial Research, National Institutes of Health, Bethesda, MD 20892, USA

[4]Department of Pharmacology, New York University School of Medicine, New York, NY 10016, USA

[5]Department of Clinical Pharmacology, Flinders University, Bedford Park, 5042, Australia

[6]The Visual Systems Group, Department of Ophthalmology and Division of Developmental Biology, Children's Hospital Research Foundation, Cincinnati, OH 45229, USA

Abstract

The developmental activities of morphogens are controlled by the gradients that they form in the extracellular matrix (ECM). In this report, we show that differences in the binding of fibroblast growth factor 7 (FGF7) and FGF10 to heparan sulfate (HS) underlie the formation of different gradients that dictate distinct activities during branching morphogenesis. Reducing the binding affinity of FGF10 for HS by mutating a single residue in its HS-binding pocket converted FGF10 into a functional mimic of FGF7 with respect to gradient formation and regulation of branching morphogenesis; in particular by causing lacrimal and salivary gland epithelium to branch rather than elongate. In contrast, mutations that reduced the affinity of the FGF10 for its receptor affected the extent, but not the nature, of the response. Our data may provide a general model for understanding how binding to HS regulates other morphogenetic gradients.

INTRODUCTION

Patterning of the mammalian embryo is regulated by gradients of morphogens, including Hedgehog (Hh), bone morphogenetic protein (BMP), transforming growth factor β (TGF-β), Wnts, and fibroblast growth factors (FGFs). Understanding how these morphogen gradients are formed and maintained is fundamental to understanding how they direct tissue patterning. Although it is well-known that many morphogens possess an affinity for heparan sulfate glycosaminoglycans (HSGAGs) in the extracellular matrix (ECM), the extent to which morphogen-HSGAG interactions contribute to morphogen gradients is not fully understood. Cellular signaling by fibroblast growth factors (FGFs) plays pleiotropic roles in mammalian development and metabolism. Based on sequence homology and phylogeny the eighteen mammalian FGFs are grouped into six subfamilies: (FGF1, 2), (FGF3, 7, 10, 22), (FGF4, 5, 6), (FGF8, 17, 18), [FGF9, 16, 20), and (FGF19, 21, 23). FGFs exert their diverse actions by

[†]Corresponding author. hmakarenk@scripps.edu.
[*]These authors contributed equally to this work.

binding to and activating FGF receptors (FGFRs) in a HS-dependent fashion (1–5). FGFs exhibit differences in their HS-binding affinities, which can impact FGF signaling at two distinct but interdependent levels: (i) they can determine the strength and duration of FGF signaling by modulating FGF-FGFR binding and dimerization; (ii) they can also dictate the radius of FGF signaling by defining the diffusion potentials of FGFs through the ECM (6). We have shown that members of the FGF19 subfamily (which includes FGF19, FGF21, and FGF23) have extremely poor affinities for HS. As a result, members of this subfamily are unique among FGFs in being able to diffuse out of the ECM to act in an endocrine fashion (7). The members of the remaining five FGF subfamilies have moderate to strong affinities for HS and accordingly act in a paracrine fashion. The example of the FGF19 subfamily suggests that more subtle differences in HS-binding affinities among paracrine FGFs may also lead to differences in their rates of diffusion in the ECM. We postulated that these differences in diffusion rate might establish FGF-specific gradients that could contribute to the different morphogenetic activities of paracrine FGFs.

To test our hypothesis, we chose FGF7 and FGF10 signaling in the context of branching morphogenesis as a model system. This selection was made based on the wealth of published data that shows that these two closely related ligands have divergent roles in branching morphogenesis despite both being produced by the mesenchyme and specifically activating FGFR2b in the epithelium (8–13). Gene knockout studies of FGF10 and FGFR2b in mice have shown that FGF10-FGFR2b signaling is required for the development of many branched organs including lungs, thyroid, pituitary, lacrimal, and salivary glands (9,11,14–17). In humans, mutations causing haploinsufficiency of the genes encoding FGF10 or FGFR2 result in autosomal dominant aplasia of lacrimal and salivary glands (ALSG: OMIM 180920 and OMIM 602115) and lacrimo-auriculo-dento-digital (LADD: OMIM 149730) syndromes (18–22). In contrast, the kidney is the only branched structure affected in FGF7-deficient mice (23). Experiments in ex vivo epithelial branching model systems including the lacrimal gland (LG) and the submandibular gland (SMG) demonstrated differences in the morphogenetic potentials of these two ligands. FGF7 induces additional budding of prebranched epithelial buds whereas FGF10 causes their elongation (12). Thus, FGF10 appears to be a stronger chemoattractant than FGF7 for LG and SMG epithelial cells (11).

In this study, we show that the different morphogenetic properties of these two ligands can be traced to a single amino acid residue difference between the HS-binding sites of FGF7 and FGF10. Mutation of Arg^{178} of FGF10 to valine, the corresponding residue in FGF7, reduced its binding to HS and converted FGF10 into FGF7 with respect to diffusion characteristics and morphogenetic activity. In particular, this single change caused FGF10 to induce branching rather than elongation of epithelial buds. Thus, our data suggest that differences in HS-binding affinity not only define whether an FGF ligand acts in an endocrine or paracrine,manner but they also distinguish the biology of different FGFs within the same subfamily. In broader terms, our study is the first to demonstrate that morphogen gradients can be established in a HS-dependent fashion and that differences in these gradients directly regulate the biology of individual morphogens. In addition, we showed that mutations in the receptor-binding region of FGF10 that decreased the affinity of FGF10 for its receptor FGFR2b affected only the extent of the response of the LG and SMG bud, but not the nature of the response (elongation vs. branching). In summary, these results clarify the distinct roles of FGF-HS interaction and FGF-FGFR binding affinity in branching morphogenesis, showing that whereas the shape of the FGF gradient regulates whether elongation or branching occurs, it is the strength of FGF10-receptor binding that regulates the extent of the response.

RESULTS

Manipulation of the diffusion of FGF10 through the ECM converts FGF10 into an FGF7 mimetic with respect to its morphogenetic potential

Two observations indicated to us that differences in their HS-binding affinities might underlie the distinct roles FGF7 and FGF10 in branching morphogenesis. First, in many branched organs, *FGF10* gene expression is restricted to a domain adjacent to the tips of epithelial buds (9,11,24). In contrast, *FGF7* gene expression in the mesenchyme is more diffuse (14,25,26). Second, the elution of FGF10 from heparin-sepharose requires higher ionic strength than does the elution of FGF7, which indicates its stronger binding to HS (27). Because HSGAGs bind to FGFs and are a major constituent of the ECM, we considered that HSGAGs might play a substantial role in influencing the diffusion of FGFs through the ECM. We postulated that differences in HSGAG-binding affinity between FGF7 and FGF10 might translate into differences in the diffusion rates of these ligands through the ECM, which would create differently shaped ligand gradients that could lead to the observed differences in their morphogenetic potential on branching organ cultures. Specifically, the ligand with the higher affinity for HS (FGF10) should diffuse only locally near its source, forming a steep gradient in which the concentration of ligand falls off sharply, whereas the ligand with the lower affinity for HS (FGF7) should diffuse more freely, forming a shallow gradient in which the concentration of ligand falls off gradually (Fig. 1, A and B).

To test whether differences in the diffusion of FGF7 and FGF10 through the ECM contribute to the divergent biology of these two ligands in branching morphogenesis, we established an LG bud explant system. LG buds from E15.5 mouse embryos were exposed to a diffusible source of FGF7 or FGF10 by presoaking heparin acrylic beads in a solution of FGF7 or FGF10 (both at 100 μg/ml) and placing them approximately 0.1 mm from the distal tip of the buds in either collagen gel or Matrigel. As previously reported (28,29), buds exposed to FGF10 elongated towards the bead with a defined distal (bud) and proximal (duct) morphology (Fig. 1, C and D). The elongation is likely a combined effect of cell proliferation (addressed later) and some directed cell migration toward the bead. In contrast, FGF7-loaded beads did not induce directional growth but instead induced branching of the bud (Fig. 1, E and F). Moreover, when we increased the distance between the bud and the FGF7- or FGF10-loaded beads, FGF10 could no longer maintain bud elongation whereas FGF7 could still induce growth (Fig. S1), supporting the idea of differential distribution of FGF7 and FGF10 within the matrix.

We then manipulated the radius of the distribution of the FGF10 ligand in the ECM by reconfiguring the experimental setting in three different ways. First, we cultured LG buds adjacent to a single bead source of FGF10 with or without soluble HS added to the matrix (Fig. 1, G to J). Soluble HS can compete for the binding of FGFs to immobilized HS proteoglycans in the ECM (30). We found that addition of soluble HS (Fig. 1, H to J) increased the radius of diffusion of FGF10 (Fig.1, I and J) and induced branching of the LG bud (Fig. 1H), whereas the FGF10-loaded bead alone induced elongation (Fig. 1G). Second, we positioned each of four FGF10-loaded beads at four positions around the bud so that it was surrounded by ligand rather than being exposed to a directional source (Fig. 1K). This induced branching instead of elongation of the bud (compare Fig. 1D with Fig. 1K). Third, we briefly (10 min) exposed LG buds to a low concentration of FGF10 (20 ng/ml) or BSA (control), washed them with PBS and growth medium, and placed them in Matrigel near an FGF10-loaded bead (Fig. 1L). Explants pretreated with FGF10 no longer elongated towards the FGF10-loaded bead but instead branched, showing small secondary buds (Fig. 1O, P). The effect of pretreatment slowly diminished until, at 48 hours, all newly formed buds of the explant extended towards the FGF10-loaded bead (Fig. 1P). Control explants exposed to a BSA solution extended towards the bead as expected (Fig. 1M, N). Taken together, these experiments suggest that the elongation response of LG buds to FGF10 was not intrinsic to the ligand itself, but rather was

due largely to its small radius of diffusion through the ECM. Moreover, exposure of both distal and proximal parts of the LG bud to FGF signals (such as occurred when we experimentally increased the diffusion range of FGF10) may be required to trigger branching instead of elongation.

Based in part on the results shown above, we developed a model to explain the different morphogenetic properties of FGF7 and FGF10. We hypothesized that the wide range of diffusion of FGF7 enables it to act on both distal and proximal parts of the developing epithelial bud, therefore inducing branching, whereas the short range of diffusion of FGF10 limits its action to the tips of the bud, thus inducing elongation (Fig. 1, A and B). Because HSGAGs bind to FGFs and are a major constituent of ECM, we further propose that differences in the HSGAG-binding affinities of FGF7 and FGF10 control the radius of their diffusion in ECM and may therefore underlie the observed differences in their morphogenetic potential on branching organ cultures.

The mutation Arg^{187}→Val converts FGF10 into a functional mimic of FGF7 with respect to gradient formation and induction of LG and SMG branching

To begin to understand the molecular basis for the observed differences in the diffusion of FGF7 and FGF10 in the ECM, we used surface plasmon resonance (SPR) analysis to compare the affinities of FGF7 and FGF10 for heparin. Heparin is a highly sulfated HSGAG that does not physiologically impact FGF-FGFR signaling but that can be used as a substitute for physiological HSGAGs in experimental settings. FGF10 bound to immobilized heparin with a higher affinity than did FGF7 (Fig. 2D). To characterize the relationship between heparin binding and FGF diffusion, the FGFs were labeled with a fluorescent dye and immobilized on heparin acrylic beads embedded in Matrigel (Fig. 2E). Diffusion of the FGFs was monitored by measuring fluorescence intensity along a line interval passing through the bead center (Fig. 2F). This analysis confirmed that FGF10 bound strongly to the matrix and diffused only a short distance from the bead, forming a short and steep gradient (Fig 2). In contrast, FGF7 diffused a considerable distance away from the bead, forming a long and shallow gradient (Fig. 2, E and F).

To further investigate the contribution of these HSGAG-dependent gradients to the divergent morphogenetic properties of FGF7 and FGF10, we engineered FGF10 molecules with FGF7-like heparin-binding sites. To this end, we modeled the interactions of FGF7 and FGF10 with heparin by superimposing the β-trefoil regions of both ligands onto that of FGF2 in the structure of a ternary FGF2-FGFR2c-heparin complex (Fig. 2, A to C) (PDB ID: 1FQ9) (5, 18). Structural analysis identified four amino acid residues in the heparin-binding site, changes in which could account for the different HS-binding affinities of the two ligands (Fig. 2, A to C). The following single mutations were introduced into the heparin binding site of FGF10: Arg^{187}→Val (R187V), Arg^{193}→Lys (R193K), Lys^{195}→Glu (K195E), and Thr^{197}→Lys (T197K) (Fig.2, B and C). In each case, the mutation substituted the amino acid residue in the heparin-binding site of FGF10 with the analogous residue in FGF7, which should impact contacts between the FGF and heparin. In particular, the R187V mutation eliminates the interaction between the positively-charged side-chain of R187 and the negatively-charged sulfate groups in heparin. Consistent with structural predictions, SPR analysis revealed a marked reduction in the binding of $FGF10^{R187V}$ to heparin relative to that of wild-type (WT) FGF10, whereas $FGF10^{R193K}$ exhibited an intermediate loss of heparin binding (Fig. 2D). With an in vitro diffusion assay, we found that $FGF10^{R187V}$ showed an almost identical pattern of diffusion to that of WT FGF7, whereas $FGF10^{R193K}$ showed increased diffusion relative to WT FGF10 but decreased diffusion compared to that of $FGF10^{R187V}$ and WT FGF7 (Fig. 2, E and F).

The availability of FGF10 molecules with FGF7-like diffusion characteristics provided us with a unique opportunity to dissect the role of differential diffusion and gradient formation in dictating the ligands' morphogenetic activities. The activities of WT and mutant FGFs were compared by two different experimental designs. In the first assay, a single mesenchyme-free epithelial LG or SMG bud was embedded in either a collagen gel or Matrigel next to an FGF-loaded heparin acrylic bead that served as a source of diffusible FGF (Fig. 2G, table S1). In the second assay, prebranched LG and SMG epithelial explants (isolated from the mesenchyme at the stage of 3 to 5 buds) were embedded within Matrigel or laminin gel, and FGFs were added to the medium surrounding the embedded explants (Fig. 3, A, B, and E). In the latter experiment, we reasoned that the different FGFs would differentially diffuse through the gel to reach the explant, reflecting their distinct HS-binding affinities (Fig 3E).

In both assays, $FGF10^{R187V}$ mimicked the function of WT FGF7 by inducing branching, whereas $FGF10^{R193K}$ and $FGF10^{T197K}$ had mixed effects (that is they induced both branching and elongation). The effect of $FGF10^{K195E}$ was similar to that of FGF10 (Fig.2G, Fig. 3, A and B, table S1). In particular, exposing the prebranched explants to an FGF with limited capacity for diffusion induced long, thin buds, whereas exposure of the explant to an FGF with greater capacity for diffusion led to the formation of short, thick buds (Fig. 3C). These data provide further evidence to support the hypothesis that differences in gradient formation account for the distinct roles of FGF7 and FGF10 in regulating branching morphogenesis.

$FGF10^{R187V}$ mimics the activity of FGF7 by inducing an FGF7-like pattern of cell proliferation in developing epithelial explants

The results that we obtained from experiments with FGF7, FGF10, and the FGF10-HS mutants suggested that these FGFs might induce different patterns of cell proliferation. To test this idea, we examined cell proliferation within LG and SMG explants exposed to the various FGFs (Fig. 3D). Cell proliferation was analyzed by measuring the incorporation of 5-bromo-2'-deoxyuridine (BrdU), which labels cells that contain newly synthesized DNA. Immunostaining for syndecan 1, which is expressed on all epithelial cells, was used to outline the epithelium. We found that WT FGF10 and $FGF10^{K195E}$, which diffuse in a limited fashion, promoted proliferation of cells that were most proximal to the source (tip), but had little or no effect on cells that were distal (stalk) from the source (Fig. 3, D to G). $FGF10^{R193K}$ and $FGF10^{T197K}$, which have only slightly reduced binding to HS relative to that of WT FGF10, activated more cells within the tip than did WT FGF10 with some increase in the proliferation of more distal cells (Fig. 3, D to G). In contrast, FGF7 and $FGF10^{R187V}$, which have reduced binding to HS and thus a much broader diffusion range than the other FGFs tested, induced the proliferation of cells that were both proximal to (tip) and distal (stalk) from the FGF source within the developing gland (Fig. 3, D, F, and G). Thus, incorporation of BrdU in SMG and LG explants (Fig. 3) indicated that the R187V mutation converted FGF10 into an FGF7-like protein. Moreover, these experiments further support the idea that exposure of both distal and proximal parts of the lacrimal bud to FGF may be both necessary and sufficient to trigger the initiation of branching.

Mutations in the receptor-binding region of FGF10 that change the strength of the FGF10-FGFR2b interaction regulate the extent, but not the nature, of epithelial explant responses

Reducing the HS-binding affinity of FGF10 by altering its heparin-binding site will decrease the ability of HS to promote binding of the mutant ligands to FGFR2b and induce receptor dimerization, which would then result in the reduced strength, duration, or both of signaling by the mutant ligands (1). Thus it is possible, that some of the differential effects that we have observed with our FGF10 HS-binding mutants are in part due to reductions in the strength or duration of interactions between these mutant FGFs and the FGFR.

To investigate how reducing the strength or duration of the interaction between FGF10 and its receptor FGFR2b might influence branching morphogenesis of LG and SMG buds, we employed previously characterized FGF10 mutants that exhibit a reduced affinity for FGFR2b and a correspondingly reduced signaling capacity (31,32). In these experiments the activities of WT FGF10 and FGF7 and of four receptor-binding mutants of FGF10, $FGF10^{D76A}$, $FGF10^{E104A}$, $FGF10^{R155A}$ and $FGF10^{R78A}$ (32), were compared by two of the assays that we have described above. In the first, the FGFs were applied on a bead adjacent to gel-embedded LG or SMG explants (Fig. 4A; see above), and in the second, the FGFs were added to the medium surrounding the embedded epithelial explants (Fig. 4B; see above). It has been previously reported that $FGF10^{D76A}$ and $FGF10^{R155A}$ strongly diminish the interaction between FGF10 and FGFR2b and dramatically decrease the mitogenic activity of FGF10 in BALB-MK mouse keratinocytes (31,32).

Our experiments showed that application of FGF10 receptor-binding mutants simply reduced the degree of elongation of the LG and SMG epithelial explants compared to that induced by WT FGF10 (Fig. 4); however, in no case did they change the elongation response into a branching response, as was observed with the FGF10 HS-binding mutants (see above). As expected, $FGF10^{R78A}$, which has the strongest impact on the strength and duration of the FGF10-FGFR2b interaction (32), did not induce epithelial elongation (Fig. 4). These data suggest that differences in the gradient, distribution, of the FGFs in the ECM and not the differences in the interactions of these ligands with receptors are responsible for the disparate effects of the FGFs on epithelial explants.

Reducing the binding of FGF10 to the ECM mimics FGF7-induced epithelial growth

To further investigate whether manipulation of the binding of WT FGF10 to the ECM influences explant growth, we pretreated the laminin gel, which contains HSPGs (13), with the enzymes heparitinase, which degrades HSGAG or chondroitinase ABC (as a control, which degrades chondroitin sulfate A, B, and C.) and then washed out the enzyme and the cleaved HSGAG before adding the FGF10 and SMG explants. As expected, removal of HSGAGs from the ECM (with heparitinase) decreased the response of FGF10, whereas treatment with chondroitinase ABC did not. Cleaving the HSGAGs with heparitinase in the presence of FGF10 released FGF10 from the ECM and resulted in growth of the explant that was similar to that observed after the application of FGF7 (Fig. 5). Importantly, application of soluble heparin together with FGF10, FGF7, or FGF10-HS mutants resulted in explant growth that was indistinguishable from that observed with FGF7 (Fig. 5 and fig. S2 A and B). As expected, pretreating the ECM with heparitinase or chondroitinase ABC had no effect on the response of the explant to FGF7 (Fig. S2 C and D). These experiments further demonstrate that differences in the gradient or distribution of the FGFs in the ECM and not differences in the interactions of these ligands with receptors are responsible for the disparate effects of the FGFs on the SMG.

$FGF10^{R187V}$ and FGF7 induce the same gene expression signature in SMG and LG explants

To assess whether the functional similarities between $FGF10^{R187V}$ and FGF7 involved induction of similar gene expression programs, we performed a genome-wide microarray analysis of isolated SMG epithelial explants and a polymerase chain reaction (PCR) array focused on genes within the mitogen-activated protein kinase (MAPK) signaling pathway in LG explants.

Genome-wide microarray analysis was performed on isolated SMG epithelial explants that were treated for 44 hrs with FGF7, FGF10, $FGF10^{R187V}$, or $FGF10^{R193K}$. The gene expression levels in each group were compared to that of FGF10, and only 278 genes out of the 29, 000 genes present in the explants (44, 000 genes on the array) were expressed at significantly

different levels compared to expression with FGF10 treatment (with more than 2-fold change in expression and $p < 0.05$ by ANOVA with Bonferroni correction). The 278 differentially expressed genes were K-means clustered into 4 groups with similar fold-changes (log2) in their levels of gene expression (Fig. 6, A and B, table S2). Genes in clusters 1 and 3 increased expression, whereas clusters 2 and 3 decreased expression, with FGF7 compared to FGF10. The fold change (log2) in expression was greater for clusters 3 and 4 compared to clusters 1 and 2. Moreover, T-test comparison between FGF10 and $FGF10^{R193K}$ only identified one gene (Lrrk1), that changed significantly (with more than 2-fold change in expression and $p < 0.05$ with Benjamini Hochberg correction). T-test comparison between FGF7 and $FGF10^{R187V}$ only identified four genes (Col18a, Sardh, Sct and Nlrp10) that changed significantly within these pairs, suggesting a high level of similarity.

The gene expression signatures induced by each of the FGFs correlated with the morphological changes that they induced in the epithelial explants (Fig. 6, A and B). The bud morphology and gene expression profile induced by $FGF10^{R187V}$ mirrored those of FGF7, whereas the gene expression profile of $FGF10^{R193K}$ was similar to that of FGF10 (Fig. 6, A and B).

We also examined the gene expression profiles of LG explants that were treated for 36 hrs with FGF7, FGF10, or $FGF10^{R187V}$ (Fig 6, C and D) with a PCR-array focused on 88 genes within the MAPK signaling pathway. The extent of gene expression after each treatment was compared to that after treatment with FGF7. Data representing the fold-change in the expression of 59 genes that gave single amplification products are shown in Fig. 6D. Relative to FGF7, the application of FGF10 caused a 2-fold or greater increase in the expression of 7 genes and a 2-fold or greater decrease in the expression of 7 genes (Fig. 6D, table S3), providing signature patterns for these two ligands. The 45 remaining genes showed less than a 2-fold change in either direction. We then asked whether the expression profile of explants treated with $FGF10^{R187V}$ was more similar to that of FGF7 or FGF10. For each of the 14 differentially expressed genes, the extent of expression in explants treated with $FGF10^{R187V}$ was more similar to that of FGF7 than that of FGF10 (Fig. 6D). This result again correlates with the effects of these FGFs on LG bud morphology (Fig. 6C). Interestingly, the gene whose expression increased most dramatically in FGF10 treated explants (more than 10-fold) was MAP2k6 (MAPK kinase 6) (Fig. 6D), which has been previously reported to play a role in the regulation of cell proliferation (33–35).

DISCUSSION

It is well known that HSGAGs play an important role in establishing the tissue distribution of various morphogens, including those of the various FGFs (36) however, the actual mechanisms by which gradients of morphogens are established in the ECM remain an area of active investigation. It has been previously proposed that gradients of FGF8 are established in the vertebrate embryo by means of mRNA degradation coupled with the directional growth of developing tissues (37). In addition, our current study together with other recent publications show that interactions of FGFs with HS play a key role in establishing FGF gradients and regulation of FGF signaling (6,38,39)

In this study, we show that manupulation of the FGF10 gradient within the ECM alteres cellular responses to FGF10 during LG and SMG branching morphogenesis. Moreover, we also showed that mutation of a single residue in the heparin-binding site of FGF10 to the corresponding residue in FGF7 converted FGF10 into a functional mimic of FGF7 with respect to HS-binding affinity, diffusion through the ECM, morphogenetic potential, and induction of gene expression. Thus, our data establish a functional link between the HS-binding affinity of an FGF, its diffusion and gradient formation characteristics, and downstream cellular responses. In contrast, attenuating the strength or duration of the FGF10 signal by reducing the affinity

of FGF10 for FGFR2b could only alter the degree of the morphogenetic response (from prominent to greatly reduced elongation). These data indicate distinct roles for FGF gradient formation and receptor affinity in regulating branching morphogenesis.

A simple explanation for how FGFs gradients instruct epithelial bud morphogenesis is that cells are triggered to proliferate wherever the FGFRs are activated. When only tip cells are activated, the tip extends; however, when stalk cells are also activated, local proliferation within the stalk leads to formation of side buds or side growth. However, the mechanisms underlying new bud formation are clearly more complex than just the activation of cell proliferation and likely involve differential activation of downstream signaling pathways in tip and stalk cells and collective cell migration (40,41). Signaling events mediated by FGFs include the activation of the phosphoinositide 3-kinase (PI3K) and Ras-MAPK, PI3 kinase, PI hydrolysis/PKC, and Rac/Cdc42 pathways, which induce signaling cascades that control cell proliferation, migration, survival, and differentiation (12,40,41). We examined changes in the expression of genes in the MAPK pathway with a targeted array and found several genes within this pathway that were differentially regulated in whole explants by the highly diffusible FGF7 and $FGF10^{R187V}$ compared to the less diffusible FGF10. Moreover, we identified one component of the pathway, MAP2k6 (MEKK6), whose expression was strongly upregulated in FGF10-treated compared to FGF7-treated explants. MEKK6 phosphorylates and activates p38 MAPK, which is a negative regulator of cell proliferation. It is possible that the greater expression of the gene encoding MEKK6 by FGF10 is due to a threshold effect whereby changes from the high local concentration of FGF10 near the bead (and thus near the tip of the bud explant) to the low concentration of FGF10 far away from the bead (and thus near the stalk of the explant) activates the MEKK6 pathway more potently than does the relatively uniform local concentration of the more diffusible FGF7. The activation of MEKK6 may also be required for FGF10-induced duct differentiation and concomitant bud elongation.

An alternative mechanism by which immobilization of growth factor by the ECM might influence FGF-mediated signaling is through cross-talk with other cell surface receptors such as integrins. Integrin-mediated signaling pathways overlap with those of FGFs and FGFRs (42–44). Moreover, FGF1 and FGF2 bind to integrins and, in the case of FGF1, the integrin-binding site overlaps with the heparin-binding site on FGF1. For FGF1, binding to integrin influences signaling events that lead to proliferation and migration (45). Binding of FGF2 to integrins induces the corecruitment of FGFR1 (46). Conceivably, altering the binding of FGF2 to HSGAGs might also alter its ability to coengage integrins. Additionally, laminin-binding β1-integrin subunits regulate the expression of *Fgfr1b*, *Fgfr2b*, and *Fgf1* during SMG development, which provides another mechanism for cross-talk between ECM engagement and the abundance of FGFRs (47). The influence of different FGF gradients on integrin-dependent signaling and morphogenesis remains to be explored.

Structure-based sequence alignment of members of other FGF subfamilies including FGF4/6, FGF8/17/18, and FGF9/16/20 reveals primary amino acid differences in the heparin-binding region, which suggest the existence of differences in HS-binding affinities among members of these subfamilies as well (1,48–50). These differences may contribute to the divergent biology of these FGFs in vivo through conferring distinct diffusion gradient potentials. Indeed, members of the FGF8 subfamily have different distributions during brain patterning, with FGF8 being sharply localized at the mid-hind brain border, whereas FGF17 and FGF18 have broader distribution patterns. Structural and functional analysis of the FGF8 isoforms FGF8a and FGF8b have shown that differences in receptor binding affinity towards the subfamily-specific receptor isoforms play a major role in the regulation of FGF signaling (51). Thus, in this case, variations in HS-binding affinity combined with differences in receptor binding affinity may provide a powerful mechanism for specifying the nonredundant activities of subfamily members.

Our studies provide strong incentives for studying the role of HS-binding in diffusion and gradient formation through the ECM by other HS-binding morphogens such as Hh, BMPs, and TGF-β. Our data also provide a model for how to apply protein engineering to manipulate diffusion and gradient formation by morphogens through the ECM with the aim of improving their biological activities. As such, our data have implications for the therapeutic use of topically or systemically applied recombinant growth factors that are required to bind to and diffuse through ECM to reach their receptor targets.

MATERIAL AND METHODS

Mice

Timed pregnant CD-1 mice (Jackson Lab) or ICR mice (Harlan) were used to obtain embryos for these studies at embryonic day 15 (E15) for lacrimal glands and E13 for submandibular glands as previously reported (11,12)..

SPR assays

Interactions between FGF ligands and heparin were studied in real time with the BIAcore 2000 system. 140 RU of biotinylated heparin (Sigma) was coupled onto one flow cell of a streptavidin chip (GE Healthcare). A second flow cell was blocked with free biotin; the response from this flow cell was subtracted from that of the heparin-coupled flow cell to serve as a control for nonspecific binding. To examine the binding of FGFs to heparin, ligands (at a concentration of 40 nM) were injected at a rate of 50 ml/min in HBS-EP buffer (0.01 M HEPES [pH 7.4], 0.15 M NaCl, 3 mM EDTA, 0.005% surfactant P20, GE Healthcare) over the biosensor chip. The association phase of interaction for each ligand was observed for four minutes after each injection, and HBS-EP was then passed over the chip for 180 seconds to observe the dissociation phase. The biosensor chip was regenerated with 1 M NaCl in 10 mM sodium acetate (pH 4.5).

Explant cultures

LG epithelium was isolated and cultured as described previously (11). An in vitro epithelial bud extension assay was performed as previously described (28,29). Single lacrimal epithelial buds or prebranched submandibular gland epithelia were separated were isolated from the surrounding mesenchyme of the glands (11,12,28) and placed inside a drop of Matrigel or collagen gel. Heparin acrylic beads (Sigma) or blue-gel beads (Bio-Rad) were loaded with 200 to 500 ng/μl of recombinant FGF10, FGF7, or individual FGF10 mutants and the bead was placed 100 to 150 μm from the anterior part of the epithelial bud. The final concentrations of the different FGFs on the beads were checked by gel electrophoresis, and the concentration of each FGF was adjusted accordingly during the loading procedure. SMG mesenchyme-free epithelial rudiments (prebranched) were prepared and cultured as described (12). SMG were treated with neutral dispase, and the epithelial structure was mechanically separated from the mesenchyme and placed in 15 μl of 3D laminin-111 (Trevigen, Gaithersburg, MD) on top of a polycarbonate filter floating on serum-free medium containing FGF10. For removal of the HSGAGs from the laminin-111 ECM, the filter was floated on 100 μl of Hepes buffer (0.01 M HEPES, pH 7.4, with 0.15 M NaCl) supplemented with 5mM $CaCl_2$ containing heparitinase or chondroitinase ABC enzymes (both at 0.02 U/ml, Seikagaku, Japan). After a 2- to 4-hour incubation at 37°C, the filter was washed extensively with medium. In some cases, heparitinase (0.02 U/ml) or heparin (0.5 ug/ml) (Celsus, Cincinnati, OH) was added directly to the medium.

BrdU labeling and detection

SMG epithelial proliferation was detected as described (12) with a BrdU Labeling Kit (Roche) and a mouse-on-mouse staining kit (M.O.M. reagents, Dako), An antibody specific for

syndecan-1 (basal membrane marker) was added (Pharmingen) following with DAPI, and the appropriate secondary antibodies. Images were obtained with a Zeiss LSM 510 confocal microscope.

Real time RT-PCR array

LG explants were exposed to FGFs and isolated from Matrigel after 24 hrs with BD Cell recovery solution. RNA was prepared with TRizol, treated with the Ambion DNA-free kit, and reverse transcribed with Roche Transcriptor and random primers. cDNA was applied to a SuperArray Biosciences MAPK signaling PCR array plate (PAMM-061) and amplification of target genes was performed with a Perkin Elmer 7300 real-time PCR system. Results of triplicate experiments were averaged. Data analysis was based on the delta-Ct method (52) and normalized to β-actin as recommended by the manufacturer (PE, Foster City CA).

Microarray

RNA samples were prepared from epithelia treated with each growth factor with a micro RNAqueous-4PCR kit (Ambion). RNA was amplified and labeled with a Low RNA input linear amplification kit, one-color (Agilent) and Agilent 44k whole mouse genome microarrays were processed and scanned with an Agilent Microarray scanner. Three independent samples were analyzed for each growth factor. Genespring GX software was used to analyze the array data.

Supplementary Material

Refer to Web version on PubMed Central for supplementary material.

Acknowledgments

H.P.M. was supported by the Neurosciences Research Foundation and by the Sjögren's Syndrome Foundation; C.T. was supported by the Sjögren's M.P.H. and V.N.P. were supported by the Intramural Research Program of the National Institute for Dental and Craniofacial Research at the National Institutes of Health; M.M., A.B. and A.V.E. were supported by R01 DE 13686.

REFERENCES AND NOTES

1. Mohammadi M, Olsen SK, Goetz R. A protein canyon in the FGF-FGF receptor dimer selects from an a la carte menu of heparan sulfate motifs. Curr Opin Struct Biol 2005;15:506–516. [PubMed: 16154740]
2. Mohammadi M, Olsen SK, Ibrahimi OA. Structural basis for fibroblast growth factor receptor activation. Cytokine Growth Factor Rev 2005;16:107–137. [PubMed: 15863029]
3. Itoh N, Ornitz DM. Functional evolutionary history of the mouse Fgf gene family. Dev Dyn 2008;237:18–27. [PubMed: 18058912]
4. Ornitz DM, Itoh N. Fibroblast growth factors. Genome Biol 2001;2 REVIEWS3005.
5. Schlessinger J, Plotnikov AN, Ibrahimi OA, Eliseenkova AV, Yeh BK, Yayon A, Linhardt RJ, Mohammadi M. Crystal structure of a ternary FGF-FGFR-heparin complex reveals a dual role for heparin in FGFR binding and dimerization. Mol Cell 2000;6:743–750. [PubMed: 11030354]
6. Harada M, Murakami H, Okawa A, Okimoto N, Hiraoka S, Nakahara T, Akasaka R, Shiraishi YI, Futatsugi N, Mizutani-Koseki Y, Kuroiwa A, Shirouzu M, Yokoyama S, Taiji M, Iseki S, Ornitz DM, Koseki H. FGF9 monomer-dimer equilibrium regulates extracellular matrix affinity and tissue diffusion. Nat Genet. 2009
7. Goetz R, Beenken A, Ibrahimi OA, Kalinina J, Olsen SK, Eliseenkova AV, Xu C, Neubert TA, Zhang F, Linhardt RJ, Yu X, White KE, Inagaki T, Kliewer SA, Yamamoto M, Kurosu H, Ogawa Y, Kuro-o M, Lanske B, Razzaque MS, Mohammadi M. Molecular insights into the klotho-dependent, endocrine mode of action of fibroblast growth factor 19 subfamily members. Mol Cell Biol 2007;27:3417–3428. [PubMed: 17339340]

8. Horowitz A, Simons M. Branching morphogenesis. Circ Res 2008;103:784–795. [PubMed: 18845818]
9. Bellusci S, Grindley J, Emoto H, Itoh N, Hogan BL. Fibroblast growth factor 10 (FGF10) and branching morphogenesis in the embryonic mouse lung. Development 1997;124:4867–4878. [PubMed: 9428423]
10. Hogan BL. Morphogenesis. Cell 1999;96:225–233. [PubMed: 9988217]
11. Makarenkova HP, Ito M, Govindarajan V, Faber SC, Sun L, McMahon G, Overbeek PA, Lang RA. FGF10 is an inducer and Pax6 a competence factor for lacrimal gland development. Development 2000;127:2563–2572. [PubMed: 10821755]
12. Steinberg Z, Myers C, Heim VM, Lathrop CA, Rebustini IT, Stewart JS, Larsen M, Hoffman MP. FGFR2b signaling regulates ex vivo submandibular gland epithelial cell proliferation and branching morphogenesis. Development 2005;132:1223–1234. [PubMed: 15716343]
13. Patel VN, Knox SM, Likar KM, Lathrop CA, Hossain R, Eftekhari S, Whitelock JM, Elkin M, Vlodavsky I, Hoffman MP. Heparanase cleavage of perlecan heparan sulfate modulates FGF10 activity during ex vivo submandibular gland branching morphogenesis. Development 2007;134:4177–4186. [PubMed: 17959718]
14. Hoffman MP, Kidder BL, Steinberg ZL, Lakhani S, Ho S, Kleinman HK, Larsen M. Gene expression profiles of mouse submandibular gland development: FGFR1 regulates branching morphogenesis in vitro through BMP- and FGF-dependent mechanisms. Development 2002;129:5767–5778. [PubMed: 12421715]
15. Izvolsky KI, Shoykhet D, Yang Y, Yu Q, Nugent MA, Cardoso WV. Heparan sulfate-FGF10 interactions during lung morphogenesis. Dev Biol 2003;258:185–200. [PubMed: 12781692]
16. Sekine K, Ohuchi H, Fujiwara M, Yamasaki M, Yoshizawa T, Sato T, Yagishita N, Matsui D, Koga Y, Itoh N, Kato S. Fgf10 is essential for limb and lung formation. Nat Genet 1999;21:138–141. [PubMed: 9916808]
17. Xu X, Weinstein M, Li C, Naski M, Cohen RI, Ornitz DM, Leder P, Deng C. Fibroblast growth factor receptor 2 (FGFR2)-mediated reciprocal regulation loop between FGF8 and FGF10 is essential for limb induction. Development 1998;125:753–765. [PubMed: 9435295]
18. Shams I, Rohmann E, Eswarakumar VP, Lew ED, Yuzawa S, Wollnik B, Schlessinger J, Lax I. Lacrimo-auriculo-dento-digital syndrome is caused by reduced activity of the fibroblast growth factor 10 (FGF10)-FGF receptor 2 signaling pathway. Mol Cell Biol 2007;27:6903–6912. [PubMed: 17682060]
19. Entesarian M, Dahlqvist J, Shashi V, Stanley CS, Falahat B, Reardon W, Dahl N. FGF10 missense mutations in aplasia of lacrimal and salivary glands (ALSG). Eur J Hum Genet 2007;15:379–382. [PubMed: 17213838]
20. Milunsky JM, Zhao G, Maher TA, Colby R, Everman DB. LADD syndrome is caused by FGF10 mutations. Clin Genet 2006;69:349–354. [PubMed: 16630169]
21. Nie X, Luukko K, Kettunen P. FGF signalling in craniofacial development and developmental disorders. Oral Dis 2006;12:102–111. [PubMed: 16476029]
22. Entesarian M, Matsson H, Klar J, Bergendal B, Olson L, Arakaki R, Hayashi Y, Ohuchi H, Falahat B, Bolstad AI, Jonsson R, Wahren-Herlenius M, Dahl N. Mutations in the gene encoding fibroblast growth factor 10 are associated with aplasia of lacrimal and salivary glands. Nat Genet 2005;37:125–127. [PubMed: 15654336]
23. Qiao J, Uzzo R, Obara-Ishihara T, Degenstein L, Fuchs E, Herzlinger D. FGF-7 modulates ureteric bud growth and nephron number in the developing kidney. Development 1999;126:547–554. [PubMed: 9876183]
24. Izvolsky KI, Zhong L, Wei L, Yu Q, Nugent MA, Cardoso WV. Heparan sulfates expressed in the distal lung are required for Fgf10 binding to the epithelium and for airway branching. Am J Physiol Lung Cell Mol Physiol 2003;285:L838–846. [PubMed: 12818887]
25. Shiratori M, Oshika E, Ung LP, Singh G, Shinozuka H, Warburton D, Michalopoulos G, Katyal SL. Keratinocyte growth factor and embryonic rat lung morphogenesis. Am J Respir Cell Mol Biol 1996;15:328–338. [PubMed: 8810636]
26. Patel VN, Rebustini IT, Hoffman MP. Salivary gland branching morphogenesis. Differentiation 2006;74:349–364. [PubMed: 16916374]

27. Luo Y, Ye S, Kan M, McKeehan WL. Structural specificity in a FGF7-affinity purified heparin octasaccharide required for formation of a complex with FGF7 and FGFR2IIIb. Journal of cellular biochemistry 2006;97:1241–1258. [PubMed: 16315317]
28. Weaver M, Dunn NR, Hogan BL. Bmp4 and Fgf10 play opposing roles during lung bud morphogenesis. Development 2000;127:2695–2704. [PubMed: 10821767]
29. Dean C, Ito M, Makarenkova HP, Faber SC, Lang RA. Bmp7 regulates branching morphogenesis of the lacrimal gland by promoting mesenchymal proliferation and condensation. Development 2004;131:4155–4165. [PubMed: 15280212]
30. Flaumenhaft R, Moscatelli D, Rifkin DB. Heparin and heparan sulfate increase the radius of diffusion and action of basic fibroblast growth factor. J Cell Biol 1990;111:1651–1659. [PubMed: 2170425]
31. Ibrahimi OA, Yeh BK, Eliseenkova AV, Zhang F, Olsen SK, Igarashi M, Aaronson SA, Linhardt RJ, Mohammadi M. Analysis of mutations in fibroblast growth factor (FGF) and a pathogenic mutation in FGF receptor (FGFR) provides direct evidence for the symmetric two-end model for FGFR dimerization. Mol Cell Biol 2005;25:671–684. [PubMed: 15632068]
32. Yeh BK, Igarashi M, Eliseenkova AV, Plotnikov AN, Sher I, Ron D, Aaronson SA, Mohammadi M. Structural basis by which alternative splicing confers specificity in fibroblast growth factor receptors. Proc Natl Acad Sci U S A 2003;100:2266–2271. [PubMed: 12591959]
33. Challen G, Gardiner B, Caruana G, Kostoulias X, Martinez G, Crowe M, Taylor DF, Bertram J, Little M, Grimmond SM. Temporal and spatial transcriptional programs in murine kidney development. Physiol Genomics 2005;23:159–171. [PubMed: 15998744]
34. Zhang R, Murakami S, Coustry F, Wang Y, de Crombrugghe B. Constitutive activation of MKK6 in chondrocytes of transgenic mice inhibits proliferation and delays endochondral bone formation. Proc Natl Acad Sci U S A 2006;103:365–370. [PubMed: 16387856]
35. Timofeev O, Lee TY, Bulavin DV. A subtle change in p38 MAPK activity is sufficient to suppress in vivo tumorigenesis. Cell Cycle 2005;4:118–120. [PubMed: 15611662]
36. Hacker U, Nybakken K, Perrimon N. Heparan sulphate proteoglycans: the sweet side of development. Nat Rev Mol Cell Biol 2005;6:530–541. [PubMed: 16072037]
37. Dubrulle J, Pourquie O. fgf8 mRNA decay establishes a gradient that couples axial elongation to patterning in the vertebrate embryo. Nature 2004;427:419–422. [PubMed: 14749824]
38. Kalinina J, Byron SA, Makarenkova HP, Olsen SK, Eliseenkova AV, Larochelle WJ, Dhanabal M, Blais S, Ornitz DM, Day LA, Neubert TA, Pollock PM, Mohammadi M. Homodimerization controls the fibroblast growth factor 9 subfamily's receptor binding and heparan sulfate-dependent diffusion in the extracellular matrix. Mol Cell Biol 2009;29:4663–4678. [PubMed: 19564416]
39. Chen Y, Mohammadi M, Flanagan JG. Graded levels of FGF protein span the midbrain and can instruct graded induction and repression of neural mapping labels. Neuron 2009;62:773–780. [PubMed: 19555646]
40. Boilly B, Vercoutter-Edouart AS, Hondermarck H, Nurcombe V, Le Bourhis X. FGF signals for cell proliferation and migration through different pathways. Cytokine Growth Factor Rev 2000;11:295–302. [PubMed: 10959077]
41. Friedl P, Hegerfeldt Y, Tusch M. Collective cell migration in morphogenesis and cancer. Int J Dev Biol 2004;48:441–449. [PubMed: 15349818]
42. Eliceiri BP, Cheresh DA. Adhesion events in angiogenesis. Curr Opin Cell Biol 2001;13:563–568. [PubMed: 11544024]
43. Mori S, Wu CY, Yamaji S, Saegusa J, Shi B, Ma Z, Kuwabara Y, Lam KS, Isseroff RR, Takada YK, Takada Y. Direct binding of integrin alphavbeta3 to FGF1 plays a role in FGF1 signaling. J Biol Chem 2008;283:18066–18075. [PubMed: 18441324]
44. Miyamoto S, Teramoto H, Gutkind JS, Yamada KM. Integrins can collaborate with growth factors for phosphorylation of receptor tyrosine kinases and MAP kinase activation: roles of integrin aggregation and occupancy of receptors. J Cell Biol 1996;135:1633–1642. [PubMed: 8978828]
45. Eliceiri BP, Klemke R, Stromblad S, Cheresh DA. Integrin alphavbeta3 requirement for sustained mitogen-activated protein kinase activity during angiogenesis. J Cell Biol 1998;140:1255–1263. [PubMed: 9490736]

46. Tanghetti E, Ria R, Dell'Era P, Urbinati C, Rusnati M, Ennas MG, Presta M. Biological activity of substrate-bound basic fibroblast growth factor (FGF2): recruitment of FGF receptor-1 in endothelial cell adhesion contacts. Oncogene 2002;21:3889–3897. [PubMed: 12032827]

47. Rebustini IT, Patel VN, Stewart JS, Layvey A, Georges-Labouesse E, Miner JH, Hoffman MP. Laminin alpha5 is necessary for submandibular gland epithelial morphogenesis and influences FGFR expression through beta1 integrin signaling. Dev Biol 2007;308:15–29. [PubMed: 17601529]

48. Hecht HJ, Adar R, Hofmann B, Bogin O, Weich H, Yayon A. Structure of fibroblast growth factor 9 shows a symmetric dimer with unique receptor- and heparin-binding interfaces. Acta Crystallogr D Biol Crystallogr 2001;57:378–384. [PubMed: 11223514]

49. Bellosta P, Iwahori A, Plotnikov AN, Eliseenkova AV, Basilico C, Mohammadi M. Identification of receptor and heparin binding sites in fibroblast growth factor 4 by structure-based mutagenesis. Mol Cell Biol 2001;21:5946–5957. [PubMed: 11486033]

50. Ye S, Luo Y, Lu W, Jones RB, Linhardt RJ, Capila I, Toida T, Kan M, Pelletier H, McKeehan WL. Structural basis for interaction of FGF-1, FGF-2, and FGF-7 with different heparan sulfate motifs. Biochemistry 2001;40:14429–14439. [PubMed: 11724555]

51. Olsen SK, Li JY, Bromleigh C, Eliseenkova AV, Ibrahimi OA, Lao Z, Zhang F, Linhardt RJ, Joyner AL, Mohammadi M. Structural basis by which alternative splicing modulates the organizer activity of FGF8 in the brain. Genes Dev 2006;20:185–198. [PubMed: 16384934]

52. Yuan JS, Wang D, Stewart CN Jr. Statistical methods for efficiency adjusted real-time PCR quantification. Biotechnol J 2008;3:112–123. [PubMed: 18074404]

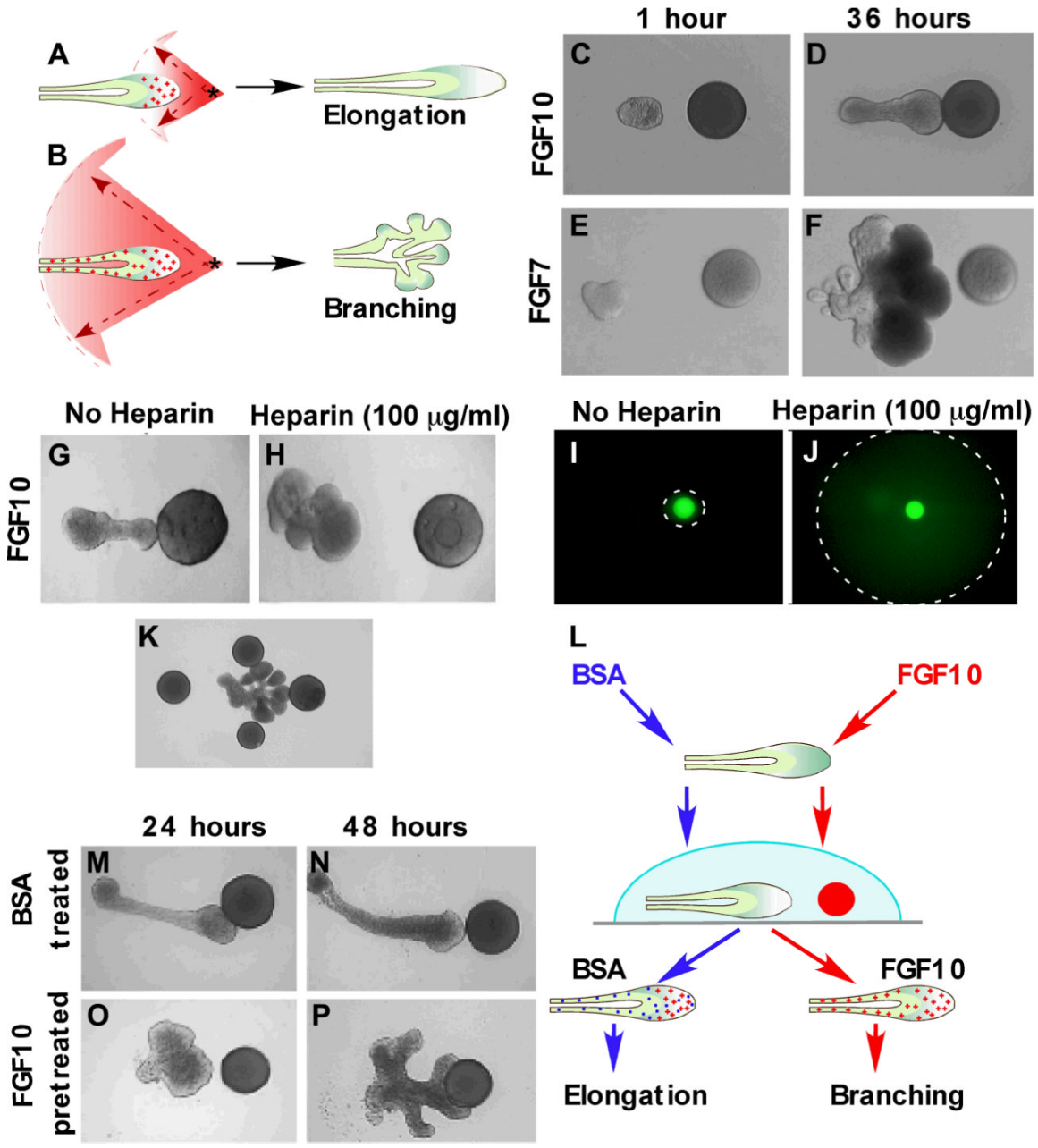

Fig. 1.

FGF gradients can regulate the morphogenesis of LG buds. (**A**, **B**) A hypothetical model of the regulation of branching morphogenesis by FGFs with different affinities for HS. FGFs applied locally (asterisk) diffuse differently depending on their affinities for HS. (A) An FGF with a high affinity for HS has restricted diffusion (red sector) through the ECM and signals only to those cells (red crosses) that are most proximal to the FGF source resulting in elongation of the bud towards the source. (**B**) An FGF with low affinity for HS has a much broader diffusion range, which leads to proliferation of cells that are proximal and distal to the FGF source, which results in branching. (**C** to **F**) Effects of FGF10 and FGF7 on the growth and migration of the isolated lacrimal bud. Within 24 hours of exposure, buds adjacent to an FGF10-loaded bead elongated towards the bead (**C, D**), whereas buds adjacent to an FGF7-loaded bead branched instead (**E, F**) (five independent experiment were performed: 8–10 explants per

condition per experiment). (**G** to **J**) Gradient formation by, and response of isolated lacrimal buds to, an FGF10-loaded bead in collagen gel in the absence (G and I) or presence (H and J) of soluble heparin. The extended FGF gradient (H) induced branching (J) instead of elongation (five experiments; 8–10 explants per condition per experiment). (**K**) Four FGF10-loaded beads placed around an LG epithelial bud induced branching (three experiments; 24 explants). (**L**) Schematic describing an experiment in which LG buds are briefly exposed to soluble FGF10 (red) or BSA (blue) prior to culture near an FGF10-loaded bead. (**M** to **P**) Short exposure of whole lacrimal buds (distal and proximal parts) to FGF10 (25 ng/ml) induced branching near the FGF10-loaded bead (L, O, and P), whereas buds treated with BSA migrated towards the bead (L, M, and N) (seven experiments performed; 8–10 explants per condition per experiment).

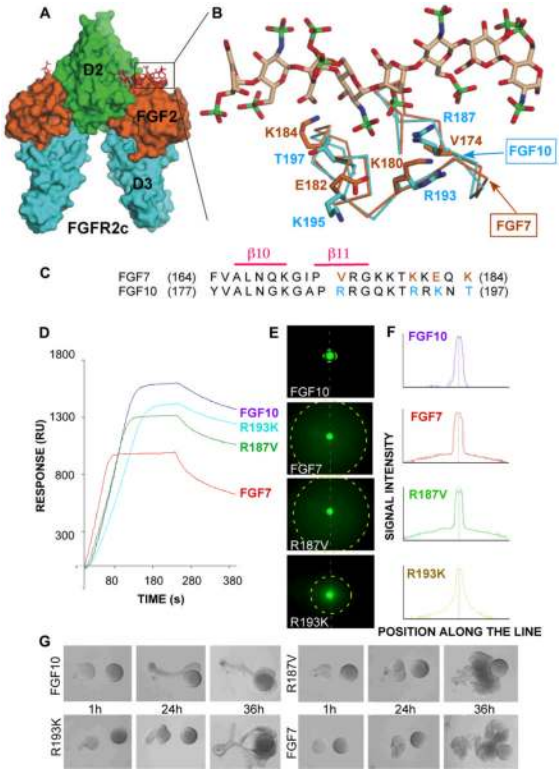

Fig. 2.

Mutations in the HS-binding domain of FGF10 change its affinity for HS, diffusion profile, and biological function. (**A**) The structure of the FGF2-FGFR2c-heparin ternary complex is shown and depicted as a surface. FGF2 is colored orange, D2 of FGFR2c is colored green, D3 of FGFR2c is colored cyan, and an 8-mer heparin molecule is colored red. The box indicates the region that is expanded and shown in (**B**), in which FGF7 and FGF10 are superimposed on the structure of FGF2; FGF2 itself is not shown. The heparin molecule has been borrowed from the FGF2-FGFR2c-heparin complex to show its interactions with FGF7 and FGF10. The FGF7 carbon backbone is colored orange, and the amino acids changes that were introduced into FGF10 have been labeled in orange. The carbon backbone of FGF10 is colored cyan, and the residues that were mutated have been labeled in cyan. The carbon backbone of heparin is colored tan. In FGF7, FGF10, and heparin, oxygen atoms are depicted as red, nitrogen atoms as blue, and sulfur atoms as green. (**C**) Sequence alignment of the heparin-binding sites of human FGF7 and FGF10. The heparin binding residues in FGF7 and FGF10 are colored in orange and cyan, respectively. (**D**) SPR analysis of the interaction of FGFs with heparin. Representative sensograms of injections of 40 nM of a given FGF over a streptavidin chip with immobilized biotinylated heparin are shown: FGF7 (red), FGF10 (blue), $FGF10^{R193K}$ (cyan), $FGF10^{R187V}$ (green). The biosensor chip response is indicated in Response Units (y-axis) as a function of time (x-axis) (five experiments was performed). (**E** to **F**) The difference in diffusion profiles of FGF10, FGF7, and FGF10-HS mutants. FGF10 formed a sharp gradient around the bead, whereas FGF7 and $FGF10^{R187V}$ diffused more freely through the matrix. $FGF10^{R193K}$ exhibited slightly increased diffusion compared to that of FGF10. (**G**) Biological responses of LG epithelial buds exposed to FGF7, FGF10, or FGF10-HS mutants on acrylic beads. $FGF10^{R187V}$ and FGF7 induced the same biological response in the bud (mainly branching), whereas FGF10 induced elongation of the bud. $FGF10^{R193K}$ had an intermediate effect; it induced both branching and elongation of the bud (15 experiments were performed).

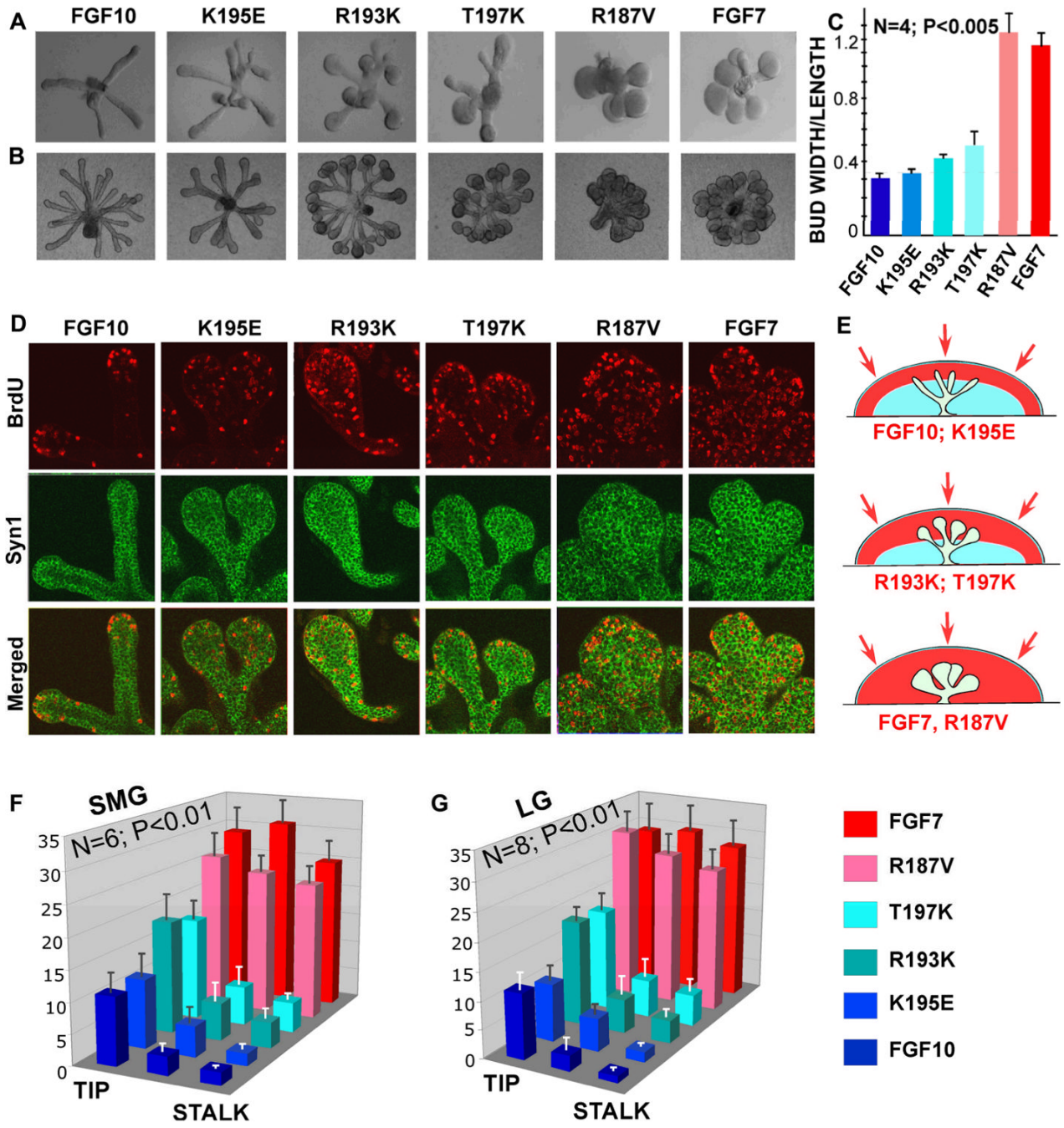

Fig. 3.

Biological responses of isolated LG and SMG epithelial explants to FGF7, FGF10, and FGF10-HS mutants in an ECM-diffusion assay. Growth responses of epithelial explants of LG (**A**) or SMG (**B**). (**C**) The morphology of the LG explant (the ratio between bud width and length) correlated with the difference in HS affinity and gradient formation of the FGF. The ratio of the width to the length of epithelial buds was determined in four independent experiments (5 to 7 explants of each kind); the Student's *t* test was used for statistical analysis. (**D**) BrdU labeling (red) of SMG explants grown in the presence of FGFs. An antibody specific for syndecan-1 (green) was used to label all of the epithelial cells. Explants exposed to the sharp gradients produced by the restricted diffusion of FGF10 and FGF10^{K195E} showed proliferating

cells only at the bud tips (which are near the interface between the gel and the medium). In contrast, $FGF10^{R193K}$ and $FGF10^{T197K}$ induced cell proliferation at the tips and also more distally in the explants. Both FGF7 and $FGF10^{R187V}$, which could diffuse freely throughout the gel, induced cell proliferation throughout the whole explant. (**E**) Different FGFs permeating into the gel are differentially captured by HS (indicated schematically in red) and are thus likely to form different gradients that elicit different cellular responses. Quantification of BrdU labeling in SMG (**F**) and LG (**G**) explants exposed to FGF ligands. Explants exposed to $FGF10^{R187V}$ showed the same labeling profile as those that were exposed to FGF7. BrdU quantification for LG and SMG explants was performed in four independent experiments (6 to 8 explants of each kind).

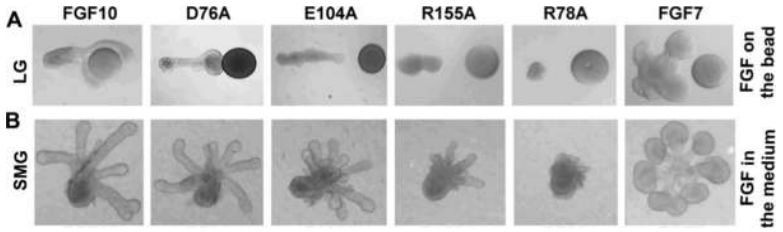

Fig. 4.

Receptor-binding mutants of FGF10 induced less elongation of LG and SMG epithelial explants than did WT-FGF10, but did not induce a switch from an elongation response to a branching response. Gel-embedded explants were exposed either to FGFs loaded on a bead (**A**) or to FGFs added to the media in a gel permeation assay (**B**). The mutant FGF10 with the strongest impact on the strength or duration of the interaction between FGF10 and FGFR2b completely blocked epithelial growth.

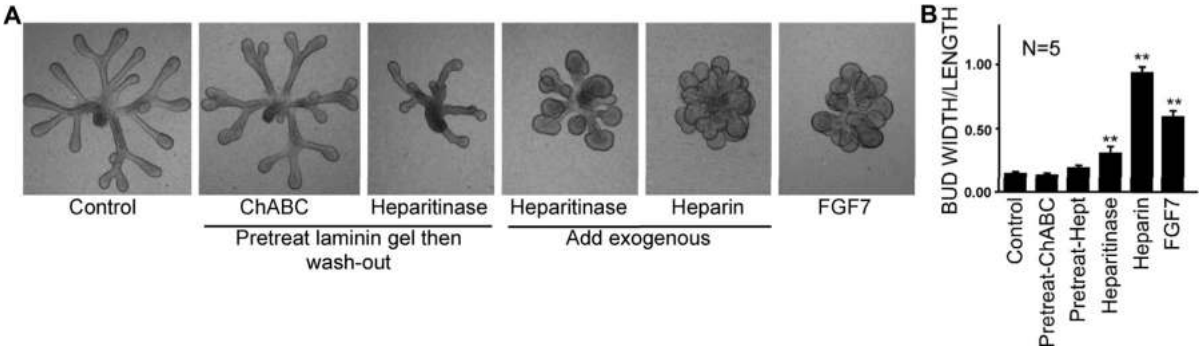

Fig. 5.

Digestion of HSGAG in the ECM or competition of FGF10 binding to the ECM with heparin changed the biological response of SMG epithelial explants to FGF10. SMG epithelia were cultured in a 3D laminin gel with FGF10 for 44 h. The 3D matrix was either pretreated with chondroitinase ABC (ChABC) or heparitinase (both at 20 U/ml) and then washed extensively with media to remove the digested GAGs and enzymes. Other groups had exogenous heparitinase (20 U/ml) or heparin (0.5 μg/ml) added to the media, with no washout of GAGs, and one group was cultured with FGF7 alone ** $p < 0.01$ as measured by ANOVA.

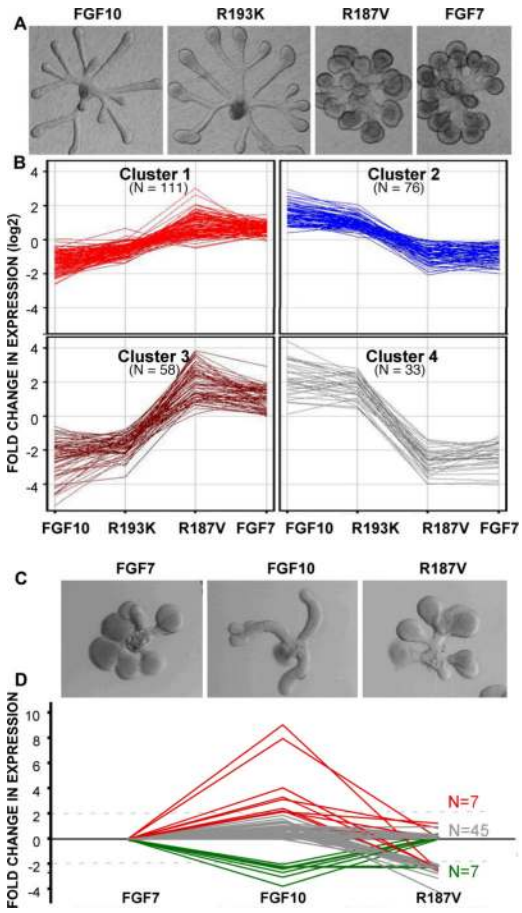

Fig. 6.

FGF10^{R187V} and FGF7 induced nearly identical gene expression profiles. (**A** and **B**) FGF7 and FGF10^{R187V} produced similar epithelial morphologies in the SMG (A) and a similar gene expression profile (B), whereas FGF10^{R193K} induced responses more similar to those elicited by FGF10 (A and B). K-means cluster analysis of changes in epithelial gene expression that were detected with an Agilent Mouse Genome Microarray after 44 hrs of culture with FGF10, FGF10^{R193K}, FGF10^{R187V}, or FGF7. (**C** and **D**) FGF7 and FGF10^{R187V} induced similar epithelial morphologies in the LG (C) and a similar gene expression profile (D). Gene expression was examined with a PCR-array focused on the MAPK signaling pathway and the expression profiles of all groups were compared to that of FGF7. Genes were clustered into 3 groups: genes that showed a greater than 2-fold increase in expression in response to FGF10 relative to that of FGF7 or FGF10^{R187V} (red), genes that showed at least a 2-fold decrease in expression in response to FGF10 relative to that of FGF7 or FGF10^{R187V} (green), and genes that showed a less than 2-fold change in expression in either direction (gray).